The Journal of Physiological Sciences (2019) 69:1041–1055
https://doi.org/10.1007/s12576-019-00724-2

ORIGINAL PAPER

The local repolarization heterogeneity in the murine pulmonary veins myocardium contributes to the spatial distribution of the adrenergically induced ectopic foci

V. M. Potekhina[1] · O. A. Averina[2] · A. A. Razumov[3] · V. S. Kuzmin[1,4] · L. V. Rozenshtraukh[5]

Received: 14 July 2019 / Accepted: 23 October 2019 / Published online: 13 November 2019

Abstract

An atrial tachyarrhythmias is predominantly triggered by a proarrhythmic activity originate from the pulmonary veins (PV) myocardial sleeves; sympathetic or adrenergic stimulation facilitates PV proarrhythmia. In the present study the electrophysiological inhomogeneity, spatiotemporal characteristics of the adrenergically induced ectopic firing and sympathetic nerves distribution have been investigated in a murine PV myocardium to clarify mechanisms of adrenergic PV ectopy. Electrically paced murine PV demonstrate atrial-like pattern of conduction and atrial-like action potentials (AP) with longest duration in the mouth of PV. The application of norepinephrine (NE), agonists of α- and β-adrenergic receptors (ARs) or intracardiac nerves stimulation induced spontaneous AP in a form of periodical bursts or continuous firing. NE- or ARs agonists-induced SAP originated from unifocal ectopic foci with predominant localization in the region surrounding PV mouth, but not in the distal portions of a murine PV myocardium. A higher level of catecholamine content and catecholamine fiber network density was revealed in the PV myocardial sleeves relative to LA appendage. However, no significant local variation of catecholamine content and fiber density was observed in the murine PV. In conclusion, PV mouth region appear to be a most susceptible to adrenergic proarrhythmia in mice. Intrinsic spatial heterogeneity of AP duration can be considered as a factor influencing localization of the ectopic foci in PV.

Keywords Pulmonary veins · Arrhythmia · Ectopic foci · Action potential · Ectopic focus

Abbreviations

AP	Action potentials
AR	Adrenergic receptors
EAD	Early afterdepolarization
DAD	Delayed afterdepolarization
DD	Diastolic depolarization
SAP	Spontaneous action potentials
RMP	Resting membrane potentials
LA	Left atria
LAA	Left atria appendage
PKA	Proteinkinase A
PV	Pulmonary veins
PNS	Postganglionic nerves stimulation
NCX	Natrium-sodium exchanger
NE	Norepinephrine
PHE	Phenylephrine
ISO	Isoproterenole

✉ V. M. Potekhina
vm-potekhina@yandex.ru

[1] Department of Human and Animal Physiology, Biological Faculty, Lomonosov Moscow State University, 1-12 Leninskie Gory, 119234 Moscow, Russia

[2] Institute of Functional Genomics, Lomonosov Moscow State University, Moscow, Russia

[3] Institute of Natural Sciences and Mathematics, Ural Federal University, Ekaterinburg, Russia

[4] Pirogov Russian National Research Medical University (RNRMU), Moscow, Russia

[5] Institute of Experimental Cardiology, National Medicine Research Cardiological Complex, Moscow, Russia

Introduction

The wall of pulmonary veins (PV) in most mammals including humans contains cardiac cells [1, 2]. The cardiomyocytes in PV form a functionally active myocardial tissue layers, so called myocardial sleeves that are electrically excitable, electrically coupled with a left atrium and demonstrate contractility [3, 4]. A number of fundamental

and clinical studies are focused on the PV myocardium electrophysiology either in laboratory animals or human since this tissue is considered recent two decades [5] as a main source of the supraventricular arrhythmias like atrial fibrillation. It is accepted that PV are proarrhythmic mainly due to two mechanisms—ectopic automaticity and re-entrant conduction [6, 7]. In addition to intrinsic proarrhythmicity, autonomic nerves play essential role in initiation and maintenance of the PV-derived tachyarrhythmia, since PV myocardium receives vast parasympathetic and sympathetic innervation [8]. It has been established previously that electric activity that origins from canine, rabbit, guinea pig or rat PV is highly dependent and facilitated by sympathetic stimulation or adrenergic receptors (AR) activation [9, 10].

Current conceptions of the atrial fibrillation suppose complex interaction between electrical ectopic activity in PV sleeves and sinoatrial node (SAN) derived excitation in atrial myocardium [6, 7]. The characterization of ectopic foci in PV is critical for understanding of tachyarrhythmia induction since the proarrhythmicity is associated with their localization in heterogeneous and highly innervated myocardium. The data regarding an origin and spatiotemporal pattern of the ectopic excitations in the PV myocardium is controversial in large animals and has not been described in small species.

A various mice strains and transgenic mouse models are widely used in cardiovascular investigations including researches aimed to the heart arrhythmias understanding. It has been demonstrated previously that PV myocardium in mice is extensively developed and a murine PV cardiac tissue is capable of generating spontaneous action potentials (AP) like in other animals; the sympathetic neurotransmitter norepinephrine (NE) has been revealed to induce spontaneous ectopic firing in PV [11]. Besides, the murine myocardium possesses by several unique characteristics like high beating rate, short AP duration typical for tachyarrhythmias. The repolarization of the AP in mice cardiac tissue is provided by ion currents I_{to}, I_{KACh}, I_{ss}, which are considered at present days as significant players in arrhythmia onset and the targets mediating effects of the antiarrhythmic drugs [12]. Nevertheless, the electrophysiology of PV, PV-derived proarrhythmic ectopic foci, the role of the distinct adrenergic receptors (ARs) activation in the murine PV ectopy initiation has not been studied sufficiently.

Therefore, present study is aimed on investigation of bioelectrical characteristics of different sites in murine PV myocardium. Also, present work is focused on elucidation of spatiotemporal characteristics and dominant localization of the ectopic foci induced in PV by the adrenergic receptors agonists or sympathetic nerves stimulation. This study, in addition, investigates the role of the sympathetic innervation distribution and electrophysiological inhomogeneity as factors affecting the spatial distribution of the ectopic automaticity sources in PV.

Materials and methods

Animals

All experimental procedures were carried out in accordance with the Guide for the Care and the Use of Laboratory Animals published by the US National Institutes of Health (NIH publication no. 85-23, revised 2010) and approved by the Ethics Committee of the MSU Biological department. Inbred male BALB/c mice weighing 20–25 g (totally $n=45$, 10 weeks old) were provided by "Scientific complex of biomedical technologies" animal plant (Moscow Region, Russia). Animals were held in the animal house for 2 weeks under a 12 h:12 h light:dark photoperiod in standard cages prior to the experiment and were fed ad libitum.

Isolation and perfusion of the pulmonary veins multicellular preparations

Prior to manipulation heparinized (100 IU/100 g, ip) mice were anesthetized with sodium pentobarbital (90 mg/kg, ip). The chest was opened, the left atria (LA) with PV, adjoined PV branches and lung lobes were separated from surrounding fascia and fat. The preparations including LA and PV (LA–PV) were rapidly excised, washed out from blood, incised and pinned with LA endocardial side up to the bottom of a 5 ml perfusion chamber filled with physiological (Tyrode) solution of the following composition (in mM): NaCl 118.0, KCl 2.7, NaH_2PO_4 2.2, $MgCl_2$ 1.2, $CaCl_2$ 1.8, $NaHCO_3$ 25.0, glucose 11.0, pH 7.4 ± 0.2 bubbled by 95% O_2 and 5% CO_2 gas mixture. The constant perfusion with flow rate of 15 ml/min at 37 °C was started immediately after preparation. Electrical pacing for rhythm maintaining was started immediately after the dissection in part of experiments. The tissue excitation was elicited by constant 2 ms pulses (with amplitude twice above the threshold) delivered by WP Instruments A320 (USA) stimulator with 200 ms intervals (5 Hz) if it was needed. A pair of the silver electrodes used for pacing was placed at the left atria appendage.

Microelectrode recording

The resting membrane potential (RMP), electrically evoked or spontaneous AP (SAP) were recorded by sharp glass microelectrodes (10–20 MΩ) filled with 3 M KCl. Warner high input impedance intracellular electrometer (IE-210, Warner Instruments, USA) was used to amplify the signals. The AP were digitized at 10 kHz sampling rate by using analog–digital converter (E-154, ADC "L-card", Russia,

www.lcard.ru) and analyzed using custom software (PowerGraph, DIsoft, Russia, www.powergraph.ru/en). Only a series of a stable impalements demonstrating AP with overshooting and fast AP upstroke velocity were accepted into account. Measurements were performed after 60 min of equilibration in various sites of PV and in left atria appendage (LAA). The action potential 90% duration (APD90) and RMP level were calculated. The AP duration was analyzed using MiniAnalysis 6.0.7 software (Synaptosoft, Fort Lee, NJ, USA, www.synaptosoft.com).

In part of experiments SAP were induced by catecholamines in quiescent murine PV preparations. In this case, SAP were recorded in a region surrounding mouth of the left PV. In cases when pacemaker-like SAP were observed the rate (mV/s) of a slow diastolic depolarization (DD) was calculated. The amplitude of SAP, most negative level of RMP over the period of firing, DD rate and bursts characteristics were calculated with aid of PowerGraph software.

Stimulation of intramural nerves

The excitation of intracardiac autonomic nerves was elicited by 100 Hz trains of rectangular pulses (0.1 ms 0.1 mA) of 3–5 s duration, which were delivered to the untreated or atropine treated (1 μM) tissue preparations surface via silver bipolar Teflon-coated electrodes located in the PV mouth region. Intramural postganglionic nerves stimulation (PNS) episodes were separated at least by 5 min periods of quiescence.

Mapping of the excitation in the pulmonary veins and atrial myocardium

The excitation was analyzed in the LA–PV with aid of optical mapping, di-4-ANEPPS-based technique in multicellular preparations, which were dissected as described previously (Fig. 1a). Optical mapping setup included a photodiodes

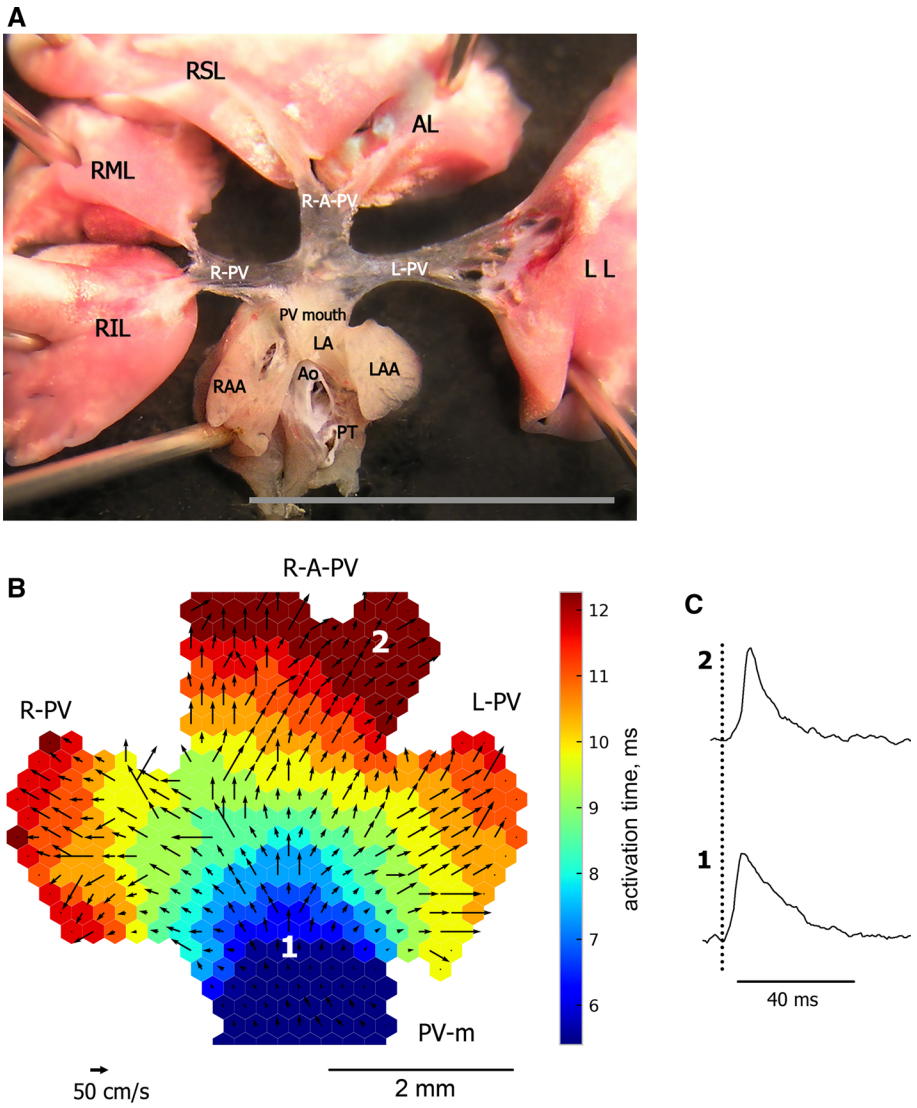

Fig. 1 **a** The macroscopic view of a murine supraventricular region and system of the pulmonary veins. LL, RML, RIL, RSL, AL: left, right middle, inferior, superior accessory lung lobes; RAA, LAA: right and left atrial appendages, RA: left atria, PT: pulmonary tract, Ao:aorta, R-PV, R-A-PV, L-PV: right, ascending and left pulmonary veins. PV mouth (PV-m): LA-PV junction region. Scale bar 5 mm. **b** Representative example of the murine PV activation map. The activation is initiated by the electrical pacing applied to atrial part of the preparation. The arrows in the activation map indicate direction of the excitation, the length of the arrows corresponds with conduction velocity. **c** Representative examples of the "optical" action potentials in PV mouth (1) and distal region of the PV (2)

array (WuTech H-469 V, Gaithersburg, MD, USA) designed for high speed data acquisition (1.63 Kfps). Macroscopic projections of the cardiac tissue preparations were transferred to the PDA with aid of the optical system including adapters and Computar V5013 (CBC Group, Japan) camera lens (focal length 50 mm, aperture ratio 1:1.3) mounted in distance of 24 mm from tissue surface. The optical system allowed project the area of 5 mm in diameter to the 464 PDA photodiodes (each 0.75 mm in diameter) which were assembled in a hexagonal array with physical aperture 19 mm (22 photodiodes in longest row). Thus, each photodiode covered the surface of 0.23 mm in diameter approximately.

It was possible to project lens field of view to the monitoring CCD camera (NexImage, Celestron, USA) via prism insertion included to the optical system. CCD camera was used to match the mapping area and PV preparation sites during experiments and data analysis.

An excitation light was emitted by three self-made green LED (520 ± 40 nm) arrays surrounding the perfusion chamber. A long-pass emission filter ($\lambda > 650$ nm) was positioned in front of the camera lens.

Potential sensitive dye di-4-ANEPPS (5 mg/mL, dissolved in DMSO) was added to the perfusion solution with final concentration 5 μmol/L and 20 min staining was carried out. The final concentration of DMSO in the solution was below 0.1%, which is acceptable for electrophysiological studies. To suppress the mechanical artifacts the electromechanical uncoupler blebbistatin was added to the perfusion solution (5 μmol/l).

Optical mapping data analysis

In all experiments fluorescent signals (optical AP) were recorded continuously for 5 s with 0.614 ms frame intervals, digitized using a data acquisition system (CardioPDA-III; RedShirtImaging, Decatur, GA, USA) and analyzed using Cardioplex (v.8.2.1, RedShirtImaging) software. The resting fluorescence was determined before each signal recording. The signals were processed via Savitsky–Golay filter using custom algorithm to remove noise and were normalized to the resting fluorescence. Also, minimal high-pass filter was applied to remove long time constant photodiode-derived basal drift. The maximum upstroke derivative (dF/dt_{max}) for each optical AP was calculated to determine the activation times in the mapped areas. Isochronic activation maps were constructed from activation times using an in-house developed software. The conduction velocity maps (CV map) and conduction direction vector field maps were reconstructed as gradients of isochronic maps using discrete gradient operator approach. The averaged CV in the PV or LA parts of the preparations were calculated as a ratio of the length of the mapped region and the activation time since the excitation wave demonstrated linear pattern. The area of an initial activation was calculated as area covered by depolarization during 1st ms after excitation beginning. The localization of the ectopic foci was defined as a center of the 1st ms activated area.

Tissue collection and processing

The capacity of catecholamines to form fluorescence adducts upon condensation with glyoxylic acid was used to estimate biogenic amines content and reveal sympathetic innervation of in the murine PV myocardium [13–15].

Murine multicellular preparations of PV and LA were isolated and washed out by Tyrode solution as described previously. After the isolation the preparations were incubated 30 min in modified PBS (NaCl 0,09 M; $Na_2HPO_4 \times 12H_2O$ 0,01 M) solution containing 2% of glyoxylic acid monohydrate and 10% sucrose, the pH of which was adjusted to 7.4 by 1 M NaOH. After the incubation the preparations were mounted on objective glasses by endocardiac side up and desiccated in 45 °C airflow during 30 min in addition to 5 min exposure in dry air thermostat at 100 °C. Desiccated tissue preparations were immersed in vaseline oil and covered by cover slips. To standardize the fluorescence outcome, the microscoping of the specimens was carried out on the next day after preparation under same room temperature and humidity.

Glyoxylic acid-induced fluorescence visualization

Confocal microscope Zeiss LSM700 with air Plan-Apochromat 20x/0,8 M27 objective was used to visualize glyoxylic acid-induced fluorescence in the immersed PV-LA preparations. The emitted fluorescence was detected in confocal mode with 0.56 μm pinhole in 405–480 nm (maximum at 435 nm) wavelengths range and was induced by diode excitation 405 nm laser. Confocal 2048 × 2048 px images included 25 stacks which covered the entire tissue samples thickness were recorded using Carl Zeiss ZEN 7.0 software.

Catecholamine-derived fluorescence and catecholamine-positive fibers quantification

Collected data were analyzed off-line by ImageJ 1.50i. software. Open-source Bio-Formats Explorer ImageJ plugins (imagej.net/Bio-Formats) were used to handle images. After background subtraction and binarization a total amount fluorescence-positive pixels was calculated as the estimation of catecholamines content in the tissue. Further processing of the images included skeletonization and skeleton analysis (imagej.net/Skeletonize3D) to estimate the extent of catecholamine-positive fibers in the local sites of PV and LA myocardial preparations. The length of the skeletonized fibers was assumed proportional to the

sympathetic innervation density [16]. All tissue preparations were stained, scanned, processed and quantified using the same protocol.

Drugs

Norepinephrine, isoproterenol (ISO), phenylephrine (PHE), atropine sulfate, glyoxylic acid were purchased from SigmaAldrich (St Louis, MO, USA). di-4-ANEPPS was purchased from Molecular Probes (Eugene, OR, USA). (±)-Blebbistatin was purchased from Tocris Bioscience (Bristol, UK).

Statistical analysis

All data in the text and figures except the original recordings are presented as mean ± SD for n experiments. GraphPad Prism 7 (GraphPad Software, USA) was used for statistical analysis of the data. The normality of the groups was tested using Shapiro–Wilk test. Hypothesis testing was carried out using a one- or two-way ANOVA (with further Dunnet correction based post hoc test for multiple comparisons in groups with repeated or independent measurements) where it was acceptable. A value $P < 0.05$ was considered as statistically significant.

Results

The conduction of the excitation in the electrically paced murine PV preparations

Both proximal and distal regions of the murine PV (including LA–PV junction zone) were excitable under the steady-state electrical pacing. All ($n = 9$) atrially paced PV demonstrated "atrial-like" anterograde consecutive, continuous conduction of the excitation lacked of wavefront disturbances resulted in a nearly simultaneous activation of the PV of different lung lobes. Murine PV also demonstrated no inexcitable zones in our experiments (Fig. 1b, c) at least in mapped extra-lung regions under steady-state pacing.

A local velocity of the conduction varied from 21 ± 5 to 110 ± 14 cm/s in different sites of the PV and demonstrated lowest value in PV mouth where it could be as low as 8 cm/s. Nevertheless, no conduction blocks were observed in PV mouth despite slow conduction as well as in others PV regions under steady-state pacing. Due to a high local variation the spatially averaged conduction velocity was statistically similar in LA/LAA and PV regions (57 ± 17 and 42 ± 18 cm/s, respectively, $n = 9$, $p > 0.1$).

The electrically evoked action potentials and resting membrane potential in the murine PV preparations

The AP with overshoot and rapid AP upstroke accompanied by a stable RMP were observed in all PV sites as well as in LA part of the preparations under the electrical pacing. However, the duration of evoked AP varied significantly among the sites of LA–PV preparations in our experiments (Fig. 2a, b). Both microelectrode recordings and optical mapping revealed longest AP in PV mouth. The APD90 accordingly to the microelectrode experiments was more than three times longer in PV mouth than in LAA—38.5 ± 5.5 and 12.3 ± 2.3 ms, respectively (Fig. 2c). In addition, the duration of the evoked AP in a right (26 ± 3.7 ms) and accessory PV (29.5 ± 4 ms) were significantly longer in comparison to LA. In contrast to APD90, the level of the resting membrane potential in LA and PV sites of the paced preparations varied nonsignificantly. The RMP was as follows: −76.6 ± 2.7 ($n = 12$), −75.8 ± 3 ($n = 9$), −76.7 ± 3.2 ($n = 9$), −78.4 ± 2.8 ($n = 7$), −76.2 ± 3.2 ($n = 7$) mV in LAA, PV mouth, left PV, right PV and ascending PV, respectively. No spontaneous AP or AP followed by early or delayed after depolarizations (EADs and DADs) were observed in paced murine LA and PV myocardium.

The ectopy induced by the adrenergic stimulation in the murine PV

In our experiments, non-paced murine PV–LA preparations were quiescent in most (24 out of 30, 80%) part of cases under control conditions and only six preparation demonstrated bursts or permanent spontaneous AP. The sympathetic neurotransmitter norepinephrine (10 μM), β-adrenoreceptors agonist isoproterenol (10 μM) and agonist of α_1-adrenoreceptors phenylephrine (10 μM) induced spontaneous electrical activity in all (100% of experiments) non-paced quiescent LA–PV preparations. An adrenergically induced spontaneous activity appeared in a form of constant firing or repetitive bursts of the SAP (Fig. 3a, b). In case of NE ($n = 8$) and ISO ($n = 10$) administration both types of spontaneous activity were observed (with repetitive bursts/constant firing ratio 5/3 and 5/5 in cases of NE and ISO application), while in case of PHE application only constant firing ($n = 6$) was initiated. The spontaneous activity induced by PHE was characterized by pacemaker-like SAP with slow diastolic depolarization (DD, 5 out of 6 experiments, Fig. 3); NE caused pacemaker-like SAP with DD in case of repetitive bursts (5 out of 5 experiments) but not in a case of constant firing. Diastolic depolarization was observed only transiently during a burst of constant firing initiation and only in a part of experiments (4 out of 10) when ISO was administered.

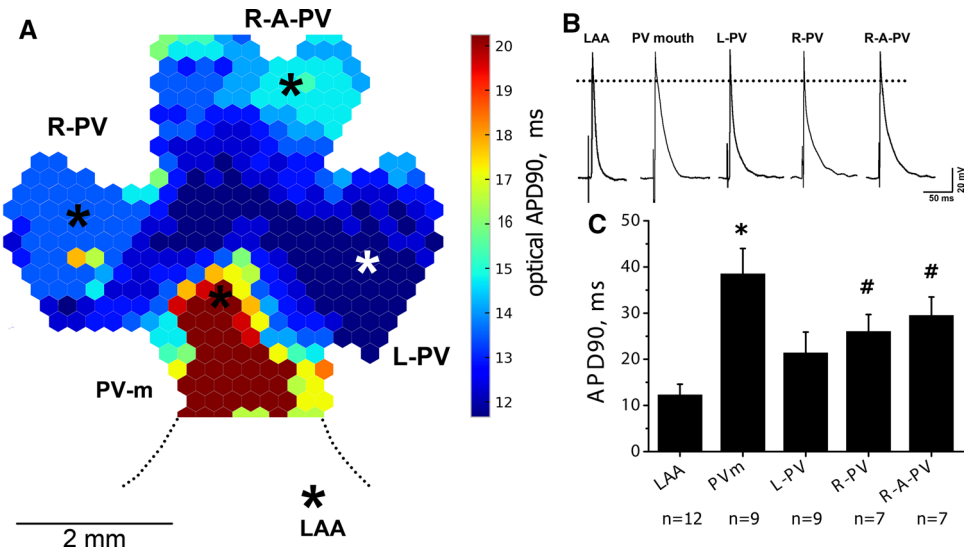

Fig. 2 Action potentials duration (APD) in the various sites of the murine left atria and pulmonary veins. **a** Representative example of the APD map of BALD/c PV tissue preparation reconstructed on the basis of the optical mapping data. The regions with most short AP shown in deep blue; with longest AP in dark red (see color scale). Time intervals between isochrones are 0.614 ms. The asterisk indicate sites of the microelectrode AP recordings. **b** Representative examples of the electrically evoked AP in murine LA and various region of PV received by sharp microelectrodes. **c** The duration of evoked AP in BALB/c LA and various sites of pulmonary veins under steady-state 5 Hz electrical pacing. * $p<0.05$ (*PV-m vs. other groups; # R-PV, R-A-PV vs. LA; ANOVA). The abbreviations are the same as in Fig. 1

The rate of NE-, ISO- and PHE-induced permanent SAP was as follows: 4.8 ± 1.8, 4.5 ± 0.4 and 2.7 ± 0.8 Hz (Fig. 4a). Therefore, NE and ISO-induced SAP was in 4–8 Hz range, which is close to a native SAN-derived rhythm in mice. However, PHE-induced automaticity demonstrated significantly lower frequency in comparison to ISO-induced SAPs ($p<0.05$).

The RMP in the quiescent murine PV tissue in control conditions was depolarized up to -59 ± 5 mV ($n=24$) unlike to the paced preparations and LA myocardium. The NE-, ISO- and PHE application was accompanied by the RMP hyperpolarization (Fig. 3c, d) that reached 23 mV (up to −82 mV). The hyperpolarization was significantly greater in response to the NE and ISO in comparison to PHE (Fig. 3c, d). It should be noted, that NE-, ISO- or PHE-induced SAP in PV were never accompanied by EADs or DADs in our experiments. Detailed characteristics of NE-, ISO- and PHE-induced spontaneous activity are shown in Fig. 4.

The ectopic foci induced by adrenergic stimulation in the murine pulmonary veins

The spontaneous AP induced in the non-paced murine LA–PV preparations under adrenoreceptors agonists application originate due to a spontaneous activation in the non-migrating myocardium regions which can be considered as sustained ectopic foci. In case of NE or PHE (5/5) application the sources of the SAP were monofocal and were localized in the region surrounding PV mouth in all experiments (6/6). The NE- and PHE-induced ectopically derived excitation was conducted continuously in a radial manner and led to the activation of both LA and distal PV myocardium. The administration of ISO also resulted in a formation of stable, spatially localized spontaneously active regions in all experiments (Figs. 5a–c, 6a–c). The ISO-induced ectopy was located predominantly in the PV mouth (4/5), however, in one case the source of the firing was found in the distal border of the right PV (Figs. 5c, right, 6c).

The area of the initial activation varied significantly from the experiment to experiment in cases of NE, PHE or ISO application. Thus, no significant differences in square of ectopic foci induced by distinct AR agonist were found. The conduction delays were observed in the PV branches in case of the ectopic activation unlike to the paced LA–PV preparations. Nevertheless, the excitation waves, originated from either NE or PHE and ISO ectopic foci were lacked of the conduction blocks; in all experiments the excitation was conducted unidirectionally without re-entry. Due to conduction delays and local conduction velocity variability the ectopic activation time of the LA-PV preparations also varied among experiments and AR agonists in range from 4 to 15.5 ms.

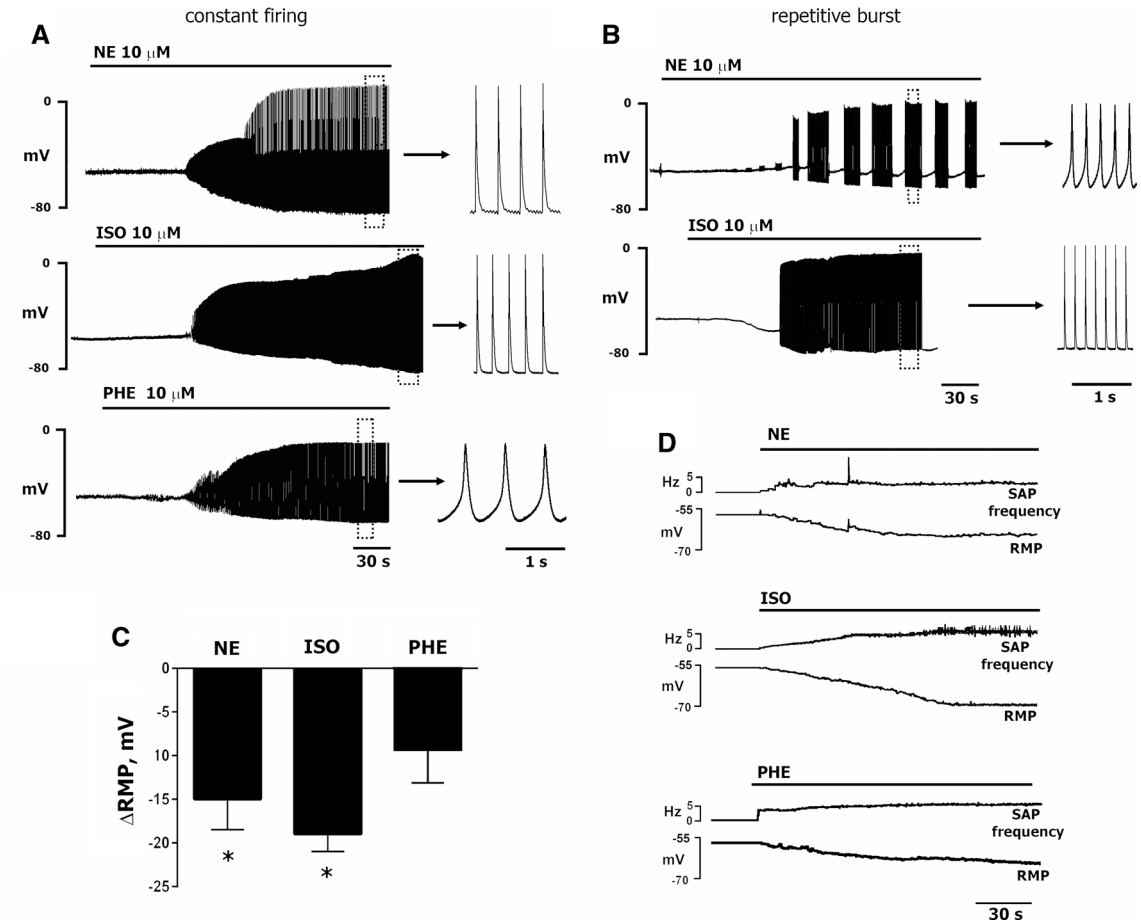

Fig. 3 Norepinephrine (NE), β-adrenoreceptors agonist isoproterenole (ISO), α-adrenoreceprors agonist phenylephrine cause periodic bursts (NA, ISO) or permanent (NA, ISO, PHE) spontaneous AP (SAP) in quiescent BALB/c pulmonary vein myocardium. **a** Representative examples of NE-, ISO- and PHE-induced permanent SAP in collapsed (left) and expanded (right) time scale. **b** Representative examples of NE- and ISO-induced repetitive bursts in different time scales. **c** NE and ISO lead to significantly more pronounced hyperpolarization of RMP in PV in comparison to PHE. * $p < 0.05$ (relative to PHE). D. NE-, ISO- or PHE-induced permanent ectopic automaticity in murine PV is accompanied by resting membrane potential (RMP) hyperpolarization

The spatial characteristics of the ectopic foci induced by postganglionic nerves stimulation in the pulmonary veins

The PNS resulted in ectopic firing initiation in the atropine-treated LA–PV preparations only in two attempts (different preparations). In these two experiments the ectopic foci were localized in the main PV trunk near the mouth of PV similarly with a case of NE or ISO administration (Figs. 5d, left, 6d). The PNS-induced automaticity sustained during 1–2 s with and the firing rate varied from maximum 12 Hz at the beginning of the burst to 3 Hz at the end of the burst (Fig. 5d, right); the pattern of PNS-induced excitation was very similar with those induced by AR agonists.

The distribution of the catecholamine-positive fibers in the murine pulmonary veins and left atria myocardium

The glyoxylic acid based staining revealed abundant catecholamine-containing fibers network in the BALB/c LA and in various sites of PV tissue (Fig. 7) including PV mouth. The total area of the catecholamine-positive fluorescence was significantly higher in the PV mouth region along with the distal PV sites in comparison to LA appendage (Fig. 7A). Similarly, the total extent of the catecholamine-positive fibers was higher in PV mouth and PV relatively to LAA (Fig. 7B). Nevertheless, no significant differences either in fluorescence area or fibers extent between PV mouth and distal PV sites were found.

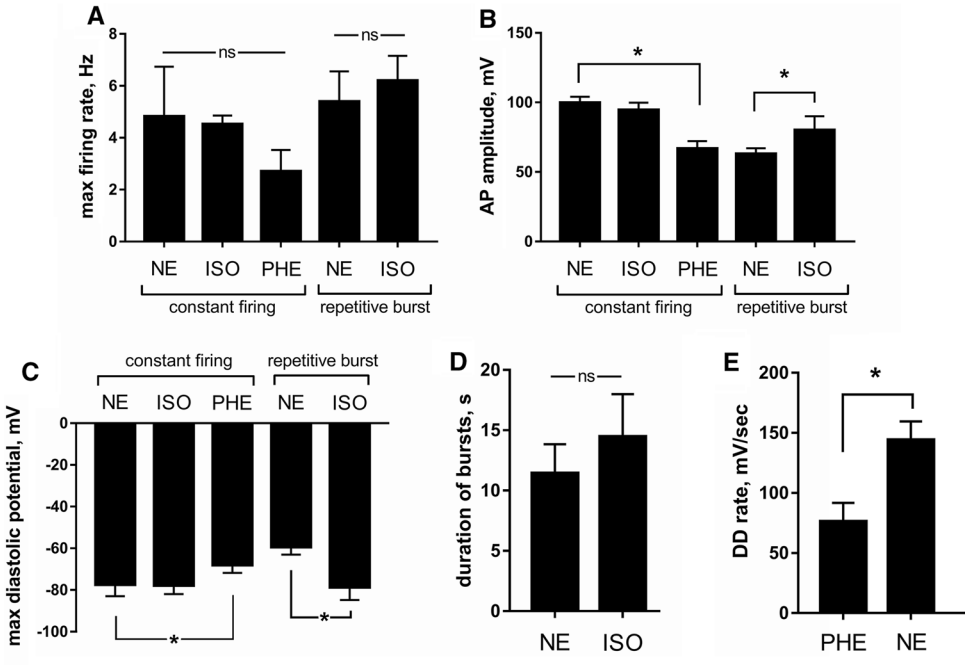

Fig. 4 Characteristics of NE-, ISO-, PHE-induced spontaneous AP and firing bursts in BALB/c pulmonary vein myocardium. **a** Maximum firing rate. **b** Amplitude of the spontaneous AP. **c** Maximal diastolic potential. **d** Averaged duration of bursts. **e** Rate of the diastolic depolarization in cases of the pacemaker-like AP induction by PHE or NE. * $p < 0.05$ (ANOVA)

Discussion

The heterogeneity of the evoked AP duration in the murine PV myocardium

The murine PV myocardium demonstrates evoked AP with typical, atrial-like waveform under the steady-state electrical pacing. In the present investigation we have demonstrated for the first time that the duration of the AP significantly differs among the regions of PV myocardium in BALB/c mice. The longest AP were observed in the tissue surrounding PV mouth (PV–LA junction) while the shortest AP appeared in the distal portions of the PV veins close to the lung lobes border. Also, the duration of the AP in the PV mouth was significantly longer than in LAA.

It has been shown previously that in other rodents species like rats and guinea pigs the duration of AP also varies among PV myocardium. The increased duration of AP in the PV mouth in respect to LA was observed also in the rat PV [17, 18]. Similarly, the duration of AP in guinea pigs PV was longer than in the LA [19]. The opposite manner of the APD distribution is common for larger animals like dogs where significantly shorter AP were observed in the PV in comparison to the atria [20]. These data allow supposing that the duration of the AP in PV and the distribution of APD in a supraventricular tissue is a species-specific parameter. Our results demonstrate that it is possible to distinguish at least two regions in the murine PV myocardium relative to the AP duration. The first region includes PV–LA junction zone or PV mouth and is characterized by long AP, while the second includes PV veins itself and shows low duration AP. The same situation was observed in rats, where a short AP in the PV sites was accompanied by significant RMP depolarization and profound acetylcholine sensitivity [17].

It has been demonstrated previously that various regions of the murine supraventricular myocardium are characterized by differences in expression of repolarizing ion currents like I_{to} and I_{KACh}. While I_{KACh} is known to be an active contributor to the cardiac repolarization only upon parasympathetic stimulation, the I_{to} acts as one of the main repolarizing currents under basal conditions in adult rodent species [21, 22]. The increased AP duration in the left posterior atrial wall (LAPW) of MF1 strain-related mice was associated with decreased I_{to} and I_{KACh} due to a reduced expression of *Kcna4* (encoding Kv1.4), *Kcnj3* (Kir3.1) and *Kcnj5* (Kir3.4) mRNA [23]. It has been hypothesized that the reduced *Kcna4*/Kv1.4/I_{to} expression contributes to a LAPW-associated proarrhythmicity in mice. In turn, an altered level of the repolarizing currents expression may results from a reduced local level of transcription factors (TF) like Nkx2-5, Tbx 5, GATA4 and others [24]. Aforementioned TFs have been demonstrated to promote expression of molecules that are critical to maintaining rapid conduction velocity (Cx40, Cx43, Nav1.5 channels), stable and negative resting membrane potential (Kir2.1/2.3 channels), i.e. electrophysiological phenotype of a working (atrial or ventricular) myocardium. It has been demonstrated that, gene expression profile, including TF is significantly altered in PV [25]. Also, the expression level of Nkx2-5 and others have been suggested to be reduced in the cardiomyocytes of PV, particularly in mice, due to an antagonism with Shox2 [26–28].

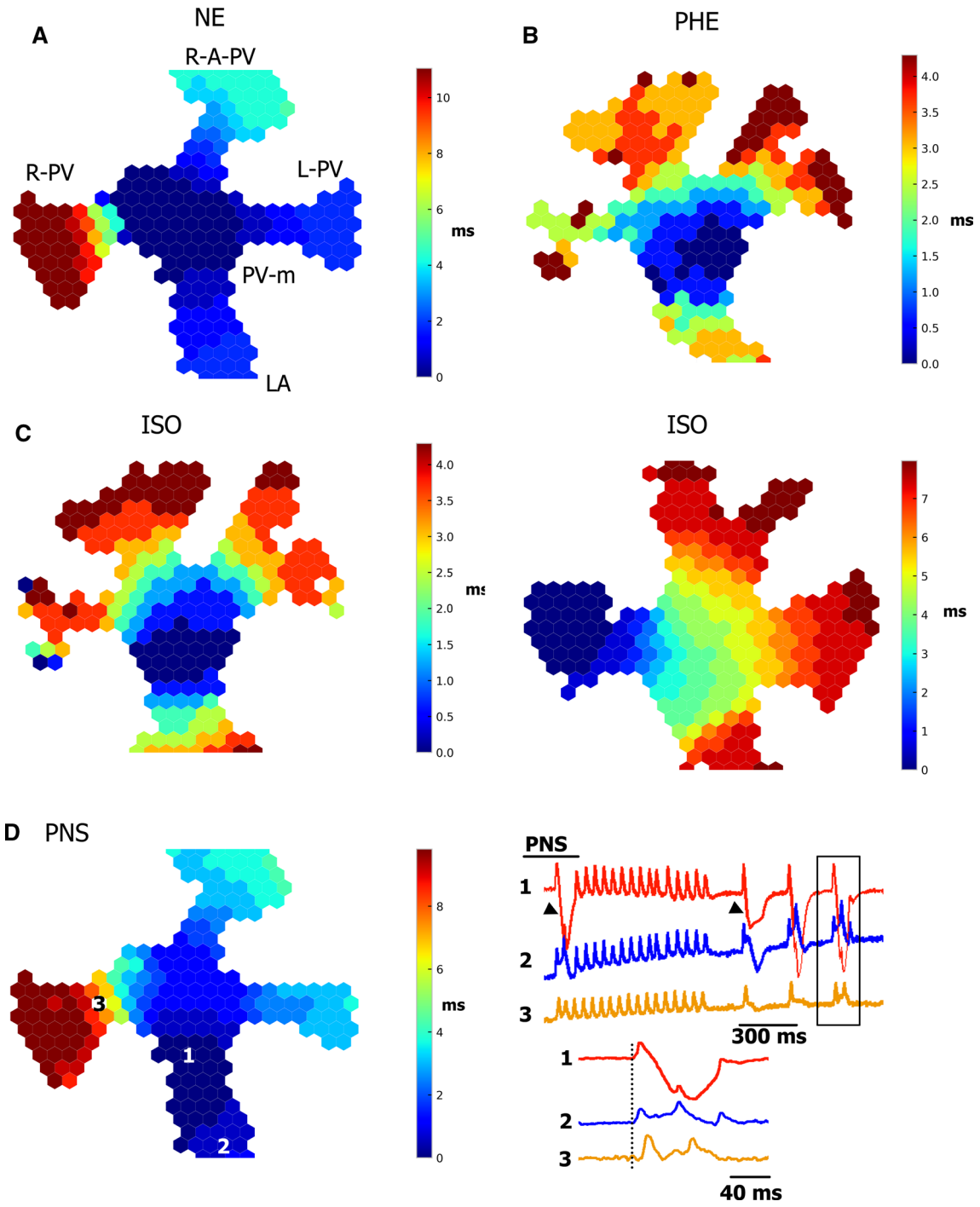

Fig. 5 Representative examples of the isochronic maps of the ectopic excitation induced by α- and β-adrenoreceptors agonists or postganglionic nerves stimulation in the BALB/c mice pulmonary veins myocardium. Norepinephrine (NE, **a**), phenylephrine (PHE, **b**) induced SAP in the region close to the PV mouth, while in response to isoproterenole (ISO) the excitation was initiated both in the PV mouth (**c**, left) or PV vein (**c**, right) sites. Postganglionic intracardiac nerves stimulation (PNS) also induced ectopic excitation in the PV mouth region (**d** left). **d,** right representative example of the sustained PNS-induced firing. The traces restricted by a black rectangle represented in the bottom of the panel but with higher time resolution. 1, 2, 3: optical AP traces from the sites indicated in **d**, left. Arrowhead: motion artifacts

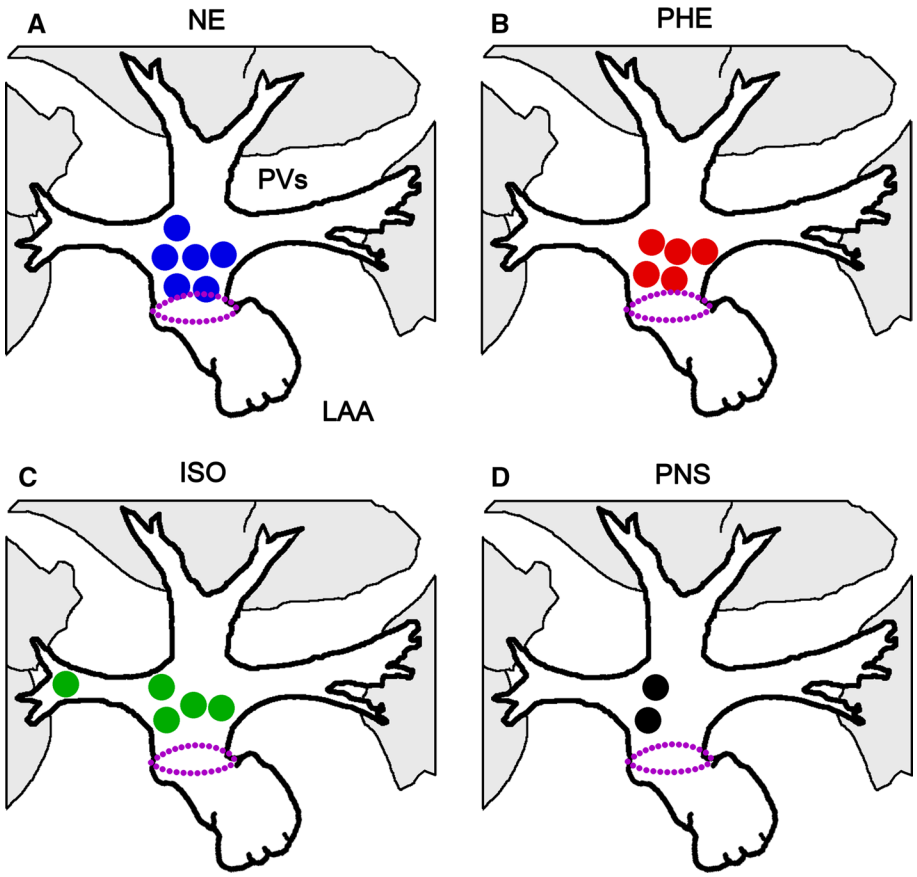

Fig. 6 The localization of the ectopic foci in the BALB/c PV myocardium. The application of the norepinephrine (NE) in PV mouth region in all cases (**a**); similarly phenylephrine-induced (PHE) ectopic automaticity was also initiated in PV mouth in all experiments (**b**); in case of isoproterenole (ISO) ectopic foci were localized in the same region (**c**) in all experiments except one. A postganglionic nerves stimulation (PNS) induced ectopic automaticity in PV tissue preparation only in two experiments (**d**). A dotted ring restricts PV mouth region. The position of the marks in the **a**–**c** panels is determined on the isochronic maps analysis as a central point of the depolarized area after the first ms of the excitation

Our results allow speculating that transmembrane repolarizing currents including I_{to}, I_{K1} and I_{ss} can be affected locally and the differences of the expression of these currents can underlie the spatial inhomogeneity of AP duration in various sites of PV myocardium in BALB/c and other mice strains. The spatial heterogeneity of the AP duration and ion currents expression can be resulted, on the other hand, from a local specificity of the transcriptional factors pattern that facilitates PV-derived ectopy.

A susceptibility of the murine PV myocardium to adrenergic ectopy

The ability of PV myocardium to generate spontaneous AP in response to adrenergic stimulation has been revealed previously in non-rodent and rodent species (rats, guinea pigs) [11, 17, 29–31]. The isolated PV cardiomyocytes from rabbits and dogs also occur highly prone to a spontaneous activity induced by adrenergic stimulation [32, 33]. To the best of our knowledge, only one investigation described NE-induced SAP in a murine PV [11]. We observed that murine PV is characterized by a low tendency to produce SAP under resting condition while ARs activation causes repetitive bursts of SAP or permanent automaticity in 100% of initially quiescent preparations. The pattern of SAP, which was observed in our experiments in BALB/c are very close those in DDY mice strain.

The ability of PV myocardium to generate SAP and ectopic automaticity has been demonstrated to be associated with several factors like altered transmembrane conductances, abnormal intracellular calcium handling, spontaneous Ca^{2+} leak and oscillations [34, 35]. For example, RyR- or IP_3-receptor dependent Ca^{2+} releases were demonstrated to trigger SAP via Na^+/Ca^{2+} exchanger (NCX) forward-mode facilitation and increase of a depolarizing component of I_{NCX} current in the rat and guinea pigs PV [30, 36]. The low density of the Kir2.X channels and inwardly rectifier I_{K1} [19], increased resting Na^+ permeability [37], enhanced chloride conduction [31] were also suggested as the mechanisms responsible for a reduced RMP and induction of SAP in PV. All aforementioned mechanisms may facilitate adrenergically induced proarrhythmic automaticity in the murine PV myocardium like in other species.

It has been shown that α_1- or combined α_1- and β-AR stimulation, but not β-AR agonists alone induced SAP in guinea pigs PV tissue [38]. In the rat PV myocardium α- or β-AR agonists alone failed to induce SAP, while the combination of the α_1-/β-agonists application caused automaticity in similar manner like NE [39]. It should be noted that PHE

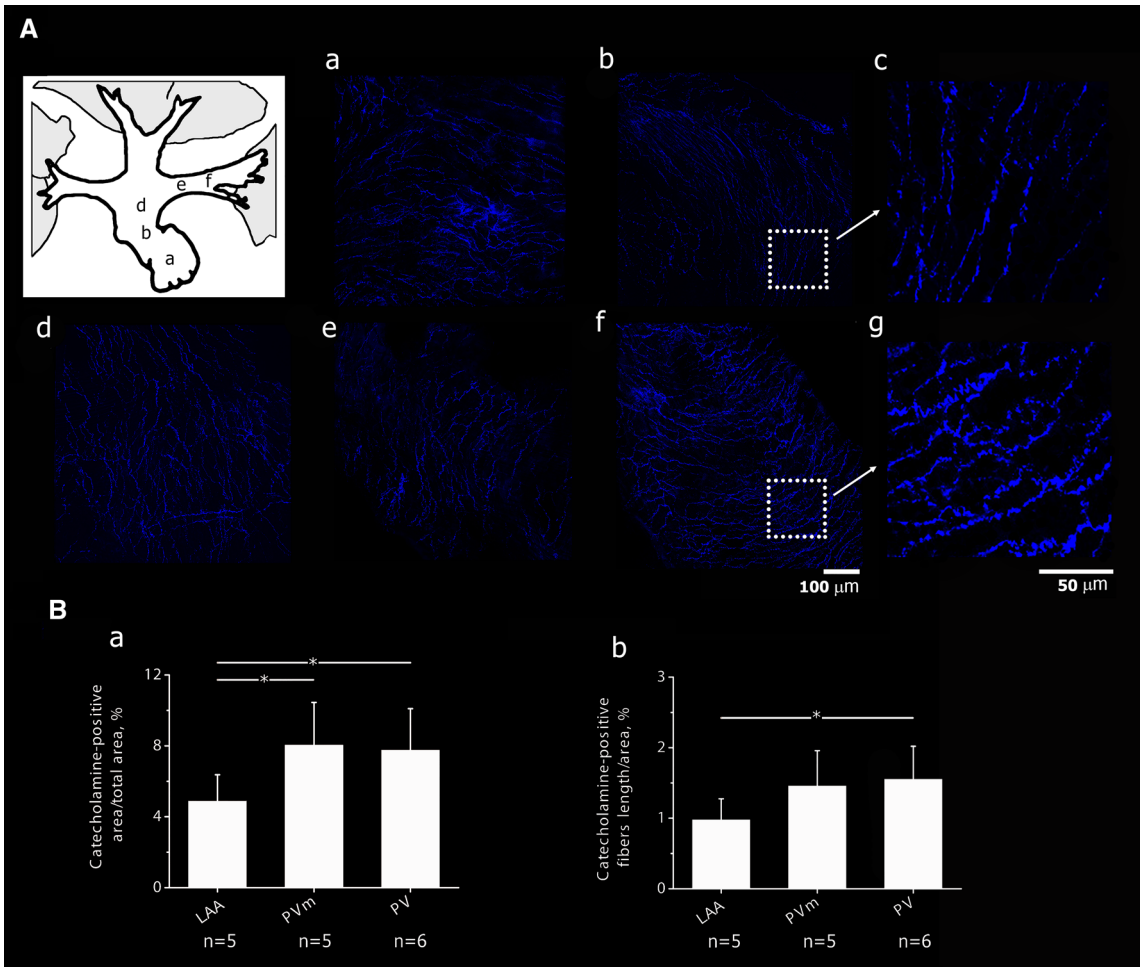

Fig. 7 **A** Representative examples of the confocal images showing catecholamine-positive fibers in the left atria appendage (**a**) and left atria wall (**b**), PV mouth (**d**), in proximal (**e**) and distal sites of the pulmonary veins (**f**, as shown in the top left inset) of BALB/c mice. **c**, **g** expanded scale of **b** and **f**. **B** The presence of the sympathetic nerves in the atria and pulmonary veins of BALB/c mice. An area of the catecholamine-derived fluorescence (**a**) and a length of the catecholamine-positive fibers (**b**) related to the total area of the images. *LAA* left atria appendage, *PV-m* PV mouth, *PV* pulmonary vein. * $p < 0.05$

and ISO applied alone induced automaticity in the murine PV in our experiments unlike others species.

Only constant firing in PV followed the administration of PHE while NE and ISO caused both permanent or periodical burst firing. A periodical termination of the firing under NE or ISO application may occur due to a higher rate of PV firing if compared to the case of PHE. Frequent APs can cause a sufficient accumulation of Na^+ in cytoplasm and stimulation of Na^+/K^+-ATPase generating hyperpolarizing current that gradually shifts PMR to a subthreshold level and temporary terminates SAP.

The agonists of α- and β-AR caused opposite RMP changes (depolarization and hyperpolarization, respectively) in rats or guinea pigs PV cardiac tissue [38, 39]. In our experiments, a nonselective ARs activation by NE as well as a selective α- or β-AR agonists application induced only RMP hyperpolarization in quiescent murine PV unlike to rats or guinea pigs. It has been demonstrated previously that α_1-AR agonists may cause RMP depolarization via I_{K1} inhibition in the rodent and non-rodent atrial myocardium [40–42]. The lack of the α1-AR-dependent RMP depolarization in BALB/c mice might results from an insensitivity of I_{K1} to PHE probably caused by a specific channel-forming Kir2.x subunits composition [43]. Norepinephrine or ISO-induced RMP hyperpolarization observed in the murine PV myocardium may be mediated by PKA activation, $[Ca^{2+}]_i$ increase, potassium inwardly rectifying currents activation (I_{KACh}) via β-ARs βγ-subunit like in others species.

In our experiments both NE (in case of repetitive bursts) and PHE-induced pacemaker-like SAP due to facilitation of diastolic depolarization; it should be noted that DD was observed in that experiments where catecholamines administration caused minimal hyperpolarization (Fig. 4). Catecholamine-induced diastolic depolarization has been

demonstrated previously in guinea pig PV myocardium where it was abolished by NCX inhibition [44]. It is established that α_1-AR activation causes significant AP plateau prolongation in the murine working myocardium due to the stimulation of NCX [45]. Therefore, it is possible to suppose that α_1-ARs induced diastolic depolarization in the murine PV myocardium in case of PHE and NE administration is caused by the stimulation of the inward component of I_{NCX} current.

Otherwise, ISO-induced SAP demonstrated an atrial-like configuration lacked of DD during steady-state period of the firing. As has been mentioned above, ISO-induced automaticity occurred at hyperpolarized RMP level since ISO administration caused a pronounced resting potential negative shift in our experiments. It is possible to speculate that in addition to I_{NCX} the hyperpolarization-activated Cl^- [31] or increased calcium-dependent Cl^- current [46] may underlie ISO-triggered SAP (as well as NE-induced permanent, DD-lacked automaticity) in the murine PV since β-ARs activation are usually accompanied by $[Ca^{2+}]_i$ elevation in cardiomyocytes.

The localization of the ectopic foci induced by adrenergic stimulation in the murine PV

The myocardial sleeves can be found in the extra-lung branches of PV, reach a deep intra-lung bifurcation of the vessels and, therefore, extensively developed in mice like in other rodents [47–49]. The cardiomyocytes both in proximal and distal parts of the murine PV are highly differentiated cardiac cells, however, the structure of the tissue is different in distinct sites of PV: a discontinuous pattern of the myocardial tissue has been shown in the intra-lung portions of the murine PV [50]. An increased interspacing of cardiomyocytes in the distal PV with fibrous tissue gussets can facilitate cells heterogeneity and promote proarrhythmicity due to an abnormal conduction. In addition, the arrhythmogenic automatic contractions due to spontaneous Ca^{2+} sparks or waves have been reported in the PV cardiac cells comprised in slice preparations from BALB/c mice intra-lung regions [34].

Aforementioned properties allowed to suppose that the distal PV are suitable sites for the proarrhythmic conduction and foci localization. Nonetheless, we observed an atrial-like continuous conduction of the excitation lengthwise PV sleeves which was free of significant abnormalities at least at extra-lung portion of the veins. Similarly, no ectopic foci were observed in distal PV both in case of NE/PHE/ISO application or postganglionic nerves stimulation in overwhelming part of our experiments. In contrast, the PV mouth, but not the PV myocardium by itself sleeves houses NE/PHE/ISO-induced monofocal, spatially localized sources of the ectopic automaticity.

Like in mice, the ectopic foci induced in a rabbit PV by NE or electrical pacing were predominantly localized in a PV mouth [51]. As has been described earlier, the cardiac tissue in the PV mouth is characterized by prolonged AP duration in contrast to other supraventricular region. It is possible that among other factors, a local electrophysiology inhomogeneity that manifests in delayed AP repolarization in PV mouth contributes to the spatial distribution of the ectopic foci in mice. We further tested whether sympathetic innervation density is associated with ectopic foci localization and electrophysiological heterogeneity in PV.

The role of catecholamine-positive fibers in the murine PV myocardium activity

In the present investigation we have described for the first time a distribution of the catecholamine-positive fibers in the PV myocardium of BALB/c mice. It is well known that the supraventricular region of a heart in mammals is abundantly innervated both by parasympathetic and sympathetic fibers. The local variations in innervation density can underlie the proarrhythmicity of the tissue.

The autonomic innervation of the myocardium is based on the so called ganglionated plexi embedded in epicardial fat pads [52]. A part of major atrial ganglionated plexi, which also described in small rodents like rat and guinea pigs [53, 54], are located close to PV-atrial junction zone and thought to play a significant role in the arrhythmia induction [55]. Several ganglionated plexi in mice surround PV mouth forming a circuit via interconnecting fibers and have nerve projections to the PV mouth and sleeves [56]. It has been demonstrated, that besides parasympathetic postganglionic neurons, the ganglionated plexi in mice and others animals demonstrate tyrosine hydroxylase immunoreactivity and contain a number of sympathetic neural elements (neurons somas and axons) [57, 58]. These observations allowed suppose an extensive adrenergic nerves network at the level of PV mouth in mice. The fibers that derive from ganglionated plexi can enhance a spatial inhomogeneity of the PV myocardium innervation. The ectopic activity can be induced predominantly near PV mouth due to increased local release of catecholamines from an abundant fibers network in vivo or in case of PNS in experiments. On the other hand, trophic effects of the sympathetic nerves can promote PV mouth myocardium susceptibility to the adrenergic proarrhythmia affecting a protein expression profile and tissue functioning [59].

Indeed, the amount of the fibers and the fluorescent area were distributed inhomogenously with a higher level in the PV myocardial sleeves relative to LA appendage. Nonetheless, our observations did not reveal significantly increased catecholamine content or catecholamine fiber network density in the area surrounding PV mouth. Thus, the localization

of the adrenergically induced foci in PV mouth cannot be attributed simply with a sympathetic hyperinnervation and increased local level of catecholamines. Our functional experiments allow speculating, that more intimate mechanisms like localized sympathetic nerves functional remodeling [60] or nerve-independent myocardium remodeling can be involved in a formation of murine PV electrophysiological heterogeneity.

Conclusion

The results of the study can be summarized as follow: murine PV myocardium demonstrates atrial-like AP and conduction under the steady-state pacing, however, local differences in AP duration indicate significant electrophysiological variations between PV mouth and distal PV. Both α- and β-AR stimulation as well as intracardiac nerves stimulation leads to ectopic foci induction localized in a tissue surrounding PV mouth. The spatial distribution of the adrenergic ectopic foci seems to be associated with a local electrophysiological inhomogeneity, rather than with increased sympathetic nerves density. Speculatively, the regional PV repolarization parameters may underlie a susceptibility and distribution of the proarrhythmic ectopic sites in non-rodent and human PV.

Funding The study is supported by RFBR 18-34-00931 grant.

References

1. Marshall J (1850) On the development of the great anterior veins in man and mammalia: including an account of certain remnants of foetal structure found in the adult, a comparative view of these great veins in the different mammalia, and an analysis of their occasional peculiarities in the human subject. Philos Trans R Soc Lond 140:133–169
2. Favaro G (1910) Contributi all'istologia umana e comparata dei vasi polmonari. Int. Monatschr. Anat. Physiol 27:375–401
3. MacLeod DP, Hunter EG (1967) The pharmacology of the cardiac muscle of the great veins of the rat. Can J Physiol Pharmacol 45(3):463–473
4. Almeida PO, Bohm CM, de Paula Carvalho M, Paes de Carvalho A (1975) The cardiac muscle in the pulmonary vein of the rat: a morphological and electrophysiological study. J Morphol 145(4):409–433
5. Haissaguerre M, Jaïs P, Shah DC, Takahashi A, Hocini M, Quiniou G, Garrigue S, Le Mouroux A, Le Métayer P, Clémenty J (1998) Spontaneous initiation of atrial fibrillation by ectopic beats originating in the pulmonary veins. N Engl J Med 339:659–666
6. Heijman J, Voigt N, Nattel S, Dobrev D (2014) Cellular and molecular electrophysiology of atrial fibrillation initiation, maintenance, and progression. Circ Res 114(9):1483–1499
7. Schotten U, Verheule S, Kirchhof P, Goette A (2011) Pathophysiological mechanisms of atrial fibrillation: a translational appraisal. Physiol Rev 91(1):265–325
8. Linz D, Elliott AD, Hohl M, Malik V, Schotten U, Dobrev D, Nattel S, Böhm M, Floras J, Lau DH, Sanders P (2019) Role of autonomic nervous system in atrial fibrillation. Int J Cardiol 287:181–188
9. Sharifov OF, Fedorov VV, Beloshapko GG, Glukhov AV, Yushmanova AV, Rosenshtraukh LV (2004) Roles of adrenergic and cholinergic stimulation in spontaneous atrial fibrillation in dogs. J Am Coll Cardiol 43(3):483–490
10. Patterson E, Po SS, Scherlag BJ, Lazzara R (2005) Triggered firing in pulmonary veins initiated by in vitro autonomic nerve stimulation. Heart Rhythm 2(6):624–631
11. Tsuneoka Y, Kobayashi Y, Honda Y, Namekata I, Tanaka H (2012) Electrical activity of the mouse pulmonary vein myocardium. J Pharmacol Sci 119:287–292
12. Schmidt C, Wiedmann F, Schweizer PA, Becker R, Katus HA, Thomas D (2012) Novel electrophysiological properties of dronedarone: inhibition of human cardiac two-pore-domain potassium (K2P) channels. Naunyn Schmiedebergs Arch Pharmacol 385(10):1003–1016
13. Axelsson S, Bjorklund A, Lindvall O (1972) Fluorescence histochemistry of biogenic monoamines. A study of the capacity of various carbonyl compounds to form fluorophores with biogenic monoamines in gas phase reactions. J Histochem Cytochem 20:435–444
14. Kyosola K, Penttila O (1977) Adrenergic innervation of the human gall bladder. Histochemistry 54:209–217
15. De la Torre JC (1980) An improved approach to histofluorescence using the SPG method for tissue monoamines. J Neurosci Methods 3:1–5
16. Sathyanesan A, Ogura T, Lin W (2012) Automated measurement of nerve fiber density using line intensity scan analysis. J Neurosci Methods 206:165–175
17. Egorov YV, Kuz'min VS, Glukhov AV, Rosenshtraukh LV (2015) Electrophysiological characteristics, rhythm, disturbances and conduction discontinuities under autonomic stimulation in the rat pulmonary vein myocardium. J Cardiovasc Electrophysiol 26:1130–1139
18. Miyauchi Y, Hayashi H, Miyauchi M, Okuyama Y, Mandel WJ, Chen PS, Karagueuzian HS (2005) Heterogeneous pulmonary vein myocardial cell repolarization implications for reentry and triggered activity. Heart Rhythm 2:1339–1345
19. Tsuneoka Y, Irie M, Tanaka Y, Sugimoto T, Kobayashi Y, Kusakabe T, Kato K, Hamaguchi S, Namekata I, Tanaka H (2017) Permissive role of reduced inwardly-rectifying potassium current density in the automaticity of the guinea pig pulmonary vein myocardium. J Pharmacol Sci 133:195–202
20. Ehrlich JR, Cha TJ, Zhang L, Chartier D, Melnyk P, Hohnloser SH, Nattel S (2003) Cellular electrophysiology of canine pulmonary vein cardiomyocytes: action potential and ionic current properties. J Physiol 551(Pt 3):801–813
21. Nerbonne JM, Kass RS (2005) Molecular physiology of cardiac repolarization. Physiol Rev 85(4):1205–1253
22. Niwa N, Nerbonne JM (2010) Molecular determinants of cardiac transient outward potassium current (I(to)) expression and regulation. J Mol Cell Cardiol 48(1):12–25
23. Holmes AP, Yu TY, Tull S, Syeda F, Kuhlmann SM, O'Brien SM, Patel P, Brain KL, Pavlovic D, Brown NA, Fabritz L, Kirchhof P (2016) A regional reduction in Ito and IKACh in the murine posterior left atrial myocardium is associated with action potential prolongation and increased ectopic activity. PLoS One. https://doi.org/10.1371/journal.pone.0154077
24. Mahida S (2014) Transcription factors and atrial fibrillation. Cardiovasc Res 101(2):194–202
25. Boutilier JK, Taylor RL, Mann T, McNamara E, Hoffman GJ, Kenny J, Dilley RJ, Henry P, Morahan G, Laing NG, Nowak KJ (2017) Gene expression networks in the murine pulmonary

myocardium provide insight into the pathobiology of atrial fibrillation. G3 (Bethesda) 7(9):2999–3017
26. Mommersteeg MT, Brown NA, Prall OW, de Gier-de Vries C, Harvey RP, Moorman AF, Christoffels VM (2007) Pitx2c and Nkx2–5 are required for the formation and identity of the pulmonary myocardium. Circ Res 101:902–909
27. Mommersteeg MT, Christoffels VM, Anderson RH, Moorman AF (2009) Atrial fibrillation: a developmental point of view. Heart Rhythm 6:1818–1824
28. Ye W, Wang J, Song Y, Yu D, Sun C, Liu C, Chen F, Zhang Y, Wang F, Harvey RP, Schrader L, Martin JF, Chen Y (2015) A common Shox2-Nkx2-5 antagonistic mechanism primes the pacemaker cell fate in the pulmonary vein myocardium and sinoatrial node. Development 142(14):2521–2532
29. Lai YJ, Huang EY, Yeh HI, Chen YL, Lin JJ, Lin CI (2008) On the mechanisms of arrhythmias in the myocardium of mXinalpha-deficient murine left atrial-pulmonary veins. Life Sci 83(7–8):272–283
30. Namekata I, Tsuneoka Y, Akiba A, Nakamura H, Shimada H, Takahara A, Tanaka H (2010) Intracellular calcium and membrane potential oscillations in the guinea pig and rat pulmonary vein myocardium. Bioimages 18:11–22
31. Okamoto Y, Kawamura K, Nakamura Y, Ono K (2014) Pathological impact of hyperpolarization-activated chloride current peculiar to rat pulmonary vein cardiomyocytes. J Mol Cell Cardiol 66:53–62
32. Chen YJ, Chen SA, Chang MS, Lin CI (2000) Arrhythmogenic activity of cardiac muscle in pulmonary veins of the dog: implication for the genesis of atrial fibrillation. Cardiovasc Res 48(2):265–273
33. Chen YJ, Chen SA, Chen YC, Yeh HI, Chang MS, Lin C (2002) Electrophysiology of single cardiomyocytes isolated from rabbit pulmonary veins: implication in initiation of focal atrial fibrillation. Basic Res Cardiol 97(1):26–34
34. Rietdorf K, Bootman MD, Sanderson MJ (2014) Spontaneous, pro-arrhythmic calcium signals disrupt electrical pacing in mouse pulmonary vein sleeve cells. PLoS One. https://doi.org/10.1371/journal.pone.0088649
35. Logantha SJ, Cruickshank SF, Rowan EG, Drummond RM (2010) Spontaneous and electrically evoked Ca^{2+} transients in cardiomyocytes of the rat pulmonary vein. Cell Calcium 48:150–160
36. Okamoto Y, Takano M, Ohba T, Ono K (2012) Arrhythmogenic coupling between the Na^{+}–Ca^{2+} exchanger and inositol 1,4,5-triphosphate receptor in rat pulmonary vein cardiomyocytes. J Mol Cell Cardiol 52:988–997
37. Malecot CO, Bredeloux P, Findlay I, Maupoil V (2015) A TTX-sensitive resting Na^{+} permeability contributes to the catecholaminergic automatic activity in rat pulmonary vein. J Cardiovasc Electrophysiol 26:311–319
38. Irie M, Tsuneoka Y, Shimobayashi M, Hasegawa N, Tanaka Y, Mochizuki S, Ichige S, Hamaguchi S, Namekata I, Tanaka H (2017) Involvement of alpha- and beta-adrenoceptors in the automaticity of the isolated guinea pig pulmonary vein myocardium. J Pharmacol Sci 133:247–253
39. Doisne N, Maupoil V, Cosnay P, Findlay I (2009) Catecholaminergic automatic activity in the rat pulmonary vein: electrophysiological differences between cardiac muscle in the left atrium and pulmonary vein. Am J Physiol Heart Circ Physiol 297:H102–H108
40. Ertl R, Jahnel U, Nawrath H, Carmeliet E, Vereecke J (1991) Differential electrophysiologic and inotropic effects of phenylephrine in atrial and ventricular heart muscle preparations from rats. Naunyn Schmiedebergs Arch Pharmacol 344(5):574–581
41. Sosunov EA, Obreztchikova MN, Anyukhovsky EP, Moïse NS, Danilo P Jr, Robinson RB, Rosen MR (2004) Mechanisms of alpha-adrenergic potentiation of ventricular arrhythmias in dogs with inherited arrhythmic sudden death. Cardiovasc Res 61(4):715–723
42. Braun AP, Fedida D, Giles WR (1992) Activation of alpha 1-adrenoceptors modulates the inwardly rectifying potassium currents of mammalian atrial myocytes. Pflugers Arch 421(5):431–439
43. Zitron E, Günth M, Scherer D, Kiesecker C, Kulzer M, Bloehs R, Scholz EP, Thomas D, Weidenhammer C, Kathöfer S, Bauer A, Katus HA, Karle CA (2008) Kir2.x inward rectifier potassium channels are differentially regulated by adrenergic alpha1A receptors. J Mol Cell Cardiol 44(1):84–94
44. Namekata I, Tsuneoka Y, Takahara A, Shimada H, Sugimoto T, Takeda K, Nagaharu M, Shigenobu K, Kawanishi T, Tanaka H (2009) Involvement of the Na(+)/Ca(2+) exchanger in the automaticity of guinea-pig pulmonary vein myocardium as revealed by SEA0400. J Pharmacol Sci 110(1):111–161
45. Tanaka H, Namekata I, Takeda K, Kazama A, Shimizu Y, Moriwaki R, Hirayama W, Sato A, Kawanishi T, Shigenobu K (2005) Unique excitation-contraction characteristics of mouse myocardium as revealed by SEA0400, a specific inhibitor of Na^{+}–Ca^{2+} exchanger. Naunyn Schmiedebergs Arch Pharmacol 371(6):526–534
46. Verkerk AO, Veldkamp MW, Bouman LN, van Ginneken AC (2000) Calcium-activated Cl(-) current contributes to delayed after depolarizations in single Purkinje and ventricular myocytes. Circ 101(22):2639–2644
47. Millino C, Sarinella F, Tiveron C et al (2000) Cardiac and smooth muscle cell contribution to the formation of the murine pulmonary veins. Dev Dyn 218:414–425
48. Stieda L (1877) Ueber quergestreifte Muskelfasern in der Wand der Lungenvenen. Arch für mikroskopische Anat 14:243–248
49. Mueller-Hoecker J, Beitinger F, Fernandez B, Bahlmann O, Assmann G, Troidl C, Dimomeletis I, Kääb S, Deindl E (2008) Of rodents and humans: a light microscopic and ultrastructural study on cardiomyocytes in pulmonary veins. Int J Med Sci 5(3):152–158
50. Kracklauer MP, Feng HZ, Jiang W, Lin JL, Lin JJ, Jin JP (2013) Discontinuous thoracic venous cardiomyocytes and heart exhibit synchronized developmental switch of troponin isoforms. FEBS J 280(3):880–891
51. Honjo H, Boyett MR, Niwa R, Inada S, Yamamoto M, Mitsui K, Horiuchi T, Shibata N, Kamiya K, Kodama I (2003) Pacing-induced spontaneous activity in myocardial sleeves of pulmonary veins after treatment with ryanodine. Circulation 107(14):1937–1943
52. Sun J, Scherlag BJ, Po SS (2014) Role of the autonomic nervous system in atrial fibrillation. In: Zipes D, Jalife J (eds) Cardiac electrophysiology: from cell to bedside, 6th edn. Elsevier, Amsterdam
53. Batulevicius D, Pauziene N, Pauza DH (2004) Key anatomic data for the use of rat heart in electrophysiological studies of the intracardiac nervous system. Medicina (Kaunas) 40(3):253–259
54. Batulevicius D, Pauziene N, Pauza DH (2005) Architecture and age-related analysis of the neuronal number of the guinea pig intrinsic cardiac nerve plexus. Ann Anat 187(3):225–243
55. Stavrakis S, Nakagawa H, Po SS, Scherlag BJ, Lazzara R, Jackman WM (2015) The role of the autonomic ganglia in atrial fibrillation. JACC Clin Electrophysiol 1(1–2):1–13
56. Zarzoso M, Rysevaite K, Milstein ML, Calvo CJ, Kean AC, Atienza F, Pauza DH, Jalife J, Noujaim SF (2013) Nerves projecting from the intrinsic cardiac ganglia of the pulmonary veins modulate sinoatrial node pacemaker function. Cardiovasc Res 99:566–575
57. Rysevaite K, Saburkina I, Pauziene N, Noujaim SF, Jalife J (2011) Pauza DH (2011) Morphologic pattern of the intrinsic ganglionated nerve plexus in mouse heart. Heart Rhythm 8(3):448–454

58. Rysevaite K, Saburkina I, Pauziene N, Vaitkevicius R, Noujaim SF, Jalife J, Pauza DH (2011) Immunohistochemical characterization of the intrinsic cardiac neural plexus in whole-mount mouse heart preparations. Heart Rhythm 8(5):731–738
59. Puzdrova VA, Kudryashova TV, Gaynullina DK, Mochalov SV, Aalkjaer C, Nilsson H, Vorotnikov AV, Schubert R, Tarasova OS (2014) Trophic action of sympathetic nerves reduces arterial smooth muscle Ca^{2+} sensitivity during early post-natal development in rats. Acta Physiol 212:128–141
60. Gardner RT, Ripplinger CM, Myles RC, Habecker BA (2016) Molecular mechanisms of sympathetic remodeling and arrhythmias. Circ Arrhythm Electrophysiol 9(2):e001359